

# Time-Resolved Photodissociation of the Molecular Ions of Propyl Phenyl Ethers

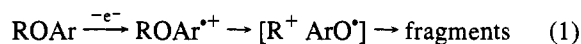
Gary H. Weddle,<sup>†,‡</sup> Robert C. Dunbar,<sup>\*,†</sup> Kyuseok Song,<sup>§,||</sup> and Thomas Hellman Morton<sup>\*,§</sup>

Contribution from the Chemistry Department, Case Western Reserve University, Cleveland, Ohio 44106, and Department of Chemistry, University of California, Riverside, California 92521-0403

Received June 16, 1994<sup>⊗</sup>

**Abstract:** The fragmentation rate of *n*-propyl phenyl ether molecular ions has been measured by time-resolved photodissociation (TRPD) in the region of 2 eV internal energy, giving first-order rate constants on the order of 10<sup>4</sup> s<sup>-1</sup>. RRKM fitting suggests a dissociation energy barrier of 1.47 eV. Decomposition of the isopropyl isomer is at least 30 times faster in this energy region. Dissociative photoionization of isopropyl phenyl ether in a supersonic jet by laser resonance-enhanced multiphoton ionization (REMPI) shows that hydrogen scrambling is insignificant for this isomer in the 4.5 eV energy range, in contrast to the earlier finding of extensive hydrogen randomization under those conditions for the *n*-propyl isomer. PhOD<sup>++</sup> is the only fragment detected in the TRPD or the REMPI of (CD<sub>3</sub>)<sub>2</sub>CHOPh. The REMPI results (guided by SCF calculations) also indicate that the two methyl groups are not equivalent in the most stable conformation of neutral isopropyl phenyl ether. A quantitative reaction coordinate is proposed for the *n*-propyl isomer dissociation, which postulates separate transition states for hydride migration and for proton transfer and an intermediate [iPr<sup>+</sup> PhO<sup>\*</sup>] ion–neutral complex. The faster dissociation of the isopropyl isomer is not consistent with the energetics predicted by UHF calculations, and it seems likely that that dissociation proceeds *via* a different mechanism.

Positive ions derived from a variety of alkyl aryl ethers decompose in the gas phase *via* the intermediacy of ion–neutral complexes, as represented in eq 1 for a radical cation.<sup>1</sup> Evidence for this mechanism derives largely from studies on rearrangements of the alkyl moiety, R<sup>+</sup>, prior to the formation of observable fragments. These rearrangements, as revealed by analysis of neutral products of the decomposition<sup>2</sup> and by isotopic labeling experiments in the mass spectrometer,<sup>1,3–8</sup> are those that would be expected of a free alkyl cation with a short ( $\approx 10^{-10}$  s) lifetime.



*n*-Propyl phenyl ether (CH<sub>3</sub>CH<sub>2</sub>CH<sub>2</sub>OPh=*n*PrOPh) represents an important example. All seven of the alkyl hydrogens become equivalent in the course of propene expulsion from its radical cation in a mass spectrometer ion source. This takes place regardless of the method by which an electron is removed from *n*PrOPh, be it electron impact,<sup>4</sup> field ionization,<sup>5</sup> or resonance-enhanced multiphoton ionization (REMPI).<sup>6,7</sup> In REMPI, absorption of two  $\approx 270$  nm photons yields the molecular ion, *n*PrOPh<sup>++</sup>. The first photon excites the neutral to its S<sub>1</sub> electronic state. Absorption of the second leads to ionization. If a third photon is absorbed, the ion can acquire enough energy to decompose on the 10<sup>-8</sup> s time scale, principally *via* expulsion of propene. Observation of intramolecular hydrogen scrambling does not depend on whether the third photon is the same color as the first two, nor are there significant differences among the different conformational isomers of *n*PrOPh.<sup>6,7</sup> By contrast, slow fragmentations are observed to give incomplete hydrogen scrambling for this ion, as manifested in metastable ion dissociations (10<sup>-5</sup> s time scale). This paper presents an experimental comparison of *n*PrOPh<sup>++</sup> with its branched isomer *i*PrOPh<sup>++</sup>. Isotopic scrambling in ionized ROPh, which takes place when R is a primary alkyl group, is scarcely observed when R is an acyclic, secondary alkyl group.<sup>8,9</sup> The appearance energies for propene expulsion from the two isomeric propyl phenyl ether radical cations (both of which give metastable ion decompositions on the microsecond time scale) have been reported to differ by nearly 0.4 eV.<sup>8</sup> Those data suggest different transition states. Here we describe a time-resolved

<sup>†</sup> Case Western Reserve University.

<sup>‡</sup> Present address: Department of Chemistry, Fairfield University, Fairfield, CT.

<sup>§</sup> University of California, Riverside.

<sup>||</sup> Present address: Korea Atomic Energy Research Institute, P.O. Box 7, Taedok Science Town, Taejeon, Korea.

<sup>⊗</sup> Abstract published in *Advance ACS Abstracts*, February 1, 1995.

(1) (a) McAdoo, D. J.; Morton, T. H. *Acc. Chem. Res.* **1993**, *26*, 295–302. (b) Morton, T. H. *Org. Mass Spectrom.* **1992**, *27*, 353–368. (c) Longevialle, P. *Mass Spectrom. Rev.* **1992**, *11*, 157–192; (d) Bowen, R. D. *Acc. Chem. Res.* **1991**, *24*, 364–371. (e) Hammerum, S. In *Fundamentals of Gas Phase Ion Chemistry*; Jennings, K. R., Ed.; Kluwer: Dordrecht, 1990; pp 379–390. (f) McAdoo, D. J. *Mass Spectrom. Rev.* **1988**, *7*, 363–393. (g) Morton, T. H. *Tetrahedron* **1982**, *38*, 3195–3243.

(2) (a) Shaler, T. A.; Morton, T. H. *J. Am. Chem. Soc.* **1994**, *116*, 9222–9226; (b) Nguyen, V.; Cheng, X.; Morton, T. H. *J. Am. Chem. Soc.* **1992**, *114*, 7127–7132. (c) Shaler, T.; Morton, T. H. *J. Am. Chem. Soc.* **1991**, *113*, 6771–6779. (d) Shaler, T.; Morton, T. H. *J. Am. Chem. Soc.* **1989**, *111*, 6868–6870; **1990**, *112*, 4090. (e) Hall, D. G.; Morton, T. H. *J. Am. Chem. Soc.* **1980**, *102*, 5686–5688. (f) Morton, T. H. *J. Am. Chem. Soc.* **1980**, *102*, 1596–1602.

(3) (a) MacLeod, J. K.; Djerassi, C. *J. Am. Chem. Soc.* **1966**, *88*, 1840–1841. (b) Yeo, A. N. H.; Djerassi, C. *J. Am. Chem. Soc.* **1972**, *94*, 482–484.

(4) Benoit, F. M.; Harrison, A. G. *Org. Mass Spectrom.* **1976**, *11*, 599–608.

(5) Borchers, F.; Levsen, K.; Beckey, H. D. *Int. J. Mass Spectrom. Ion Phys.* **1976**, *21*, 125–132.

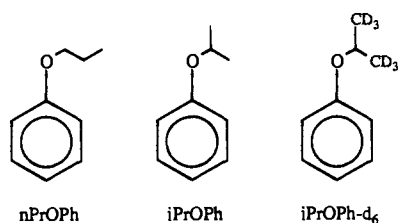
(6) Chronister, E. L.; Morton, T. H. *J. Am. Chem. Soc.* **1990**, *112*, 133–139.

(7) Song, K.; van Eijk, A.; Shaler, T. A.; Morton, T. H. *J. Am. Chem. Soc.* **1994**, *116*, 4455–4460.

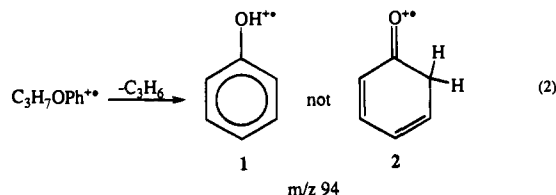
(8) (a) Blanchette, M. C.; Holmes, J. L.; Lossing, F. P. *Org. Mass Spectrom.* **1989**, *24*, 673–678. (b) Harnish, D.; Holmes, J. L. *J. Am. Chem. Soc.* **1991**, *113*, 9729–9734.

(9) (a) Sozzi, G.; Audier, H. E.; Mourges, P.; Milliet, A. *Org. Mass Spectrom.* **1987**, *22*, 746–747. (b) Kondrat, R. W.; Morton, T. H. *Org. Mass Spectrom.* **1988**, *23*, 555–557.

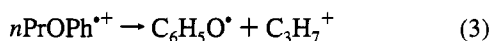
laser photodissociation (TRPD) study of the low-energy fragmentation kinetics of the two propyl phenyl ethers, which supports that inference. TRPD offers an accurate and conve-



nient method for measuring dissociation rates, from which intrinsic barrier heights can be extracted. The results are interpreted with the aid of REMPI experiments and SCF calculations. We conclude that the decomposition rates of  $n\text{PrOPh}^{+\bullet}$  and of  $i\text{PrOPh}^{+\bullet}$  are limited by different kinds of barriers. The lowest-energy decomposition channel for ionized propyl phenyl ethers corresponds to loss of propene to give an ion with the elemental composition of phenol, as represented in eq 2. The product ion from  $n\text{PrOPh}$  has been demonstrated<sup>10</sup> to have the structure phenol<sup>+\bullet</sup>, **1**, which can be distinguished from the isomeric 1,5-hydrogen rearrangement product, **2**.<sup>10,11</sup> No ion **2** has been detected from  $n\text{PrOPh}^{+\bullet}$ , either from



decompositions that take place in the ion source or among the products of metastable ion fragmentations. Fragmentation to propyl ion is also a low-energy channel, as portrayed in eq 3. In REMPI at low power densities the branching ratio for the major primary decomposition pathways (propene expulsion: propyl cation expulsion =  $m/z$  94: $m/z$  43  $\approx$  15:1) does not depend on the temperature of the neutral precursor. A gaseous sample at 300 K<sup>6</sup> gives a result very much the same as REMPI on a single conformational isomer in a supersonic free jet expansion at 30 K.<sup>7</sup>



For  $n\text{PrOPh}$  the thermodynamic threshold for eq 2 corresponds to absorption of two 275 nm photons, so decomposition is (in principle) possible following absorption of two 270 nm photons. However, no fragmentation is observed in REMPI mass spectra until a third photon is absorbed. This reflects the existence of a substantial kinetic shift, as is to be expected. The reported onset of metastable ion decompositions corresponding to eq 2 is 1.0 eV above the thermodynamic threshold, which includes whatever energy increment is necessary for eq 2 to be observable on the metastable time scale.

The present study has been designed to address three issues. The first is to provide a measurement of the barrier to eq 2 by monitoring decomposition rate as a function of ion internal energy. The second issue is the comparison of  $i\text{PrOPh}$  with  $n\text{PrOPh}$ . From its REMPI excitation spectrum and SCF calculations we infer that the two methyl groups are not equivalent in the most stable conformation of neutral  $i\text{PrOPh}$ .

(10) Maquestiau, A.; Flammang, R.; Pauwels, P.; Vallet, P.; Meyrant, P. *Org. Mass Spectrom.* **1982**, *17*, 643.

(11) Turecek, F.; Drinkwater, D. E.; Maquestiau, A.; McLafferty, F. W. *Org. Mass Spectrom.* **1989**, *24*, 669–672.

Therefore, we surmise that all six methyl hydrogens ought not to be taken as equivalent in propene expulsion from  $i\text{PrOPh}^{+\bullet}$ . Nevertheless, it turns out that the isopropyl isomer decomposes very much faster than the  $n$ -propyl ion. The third issue deals with isotopic scrambling in  $i\text{PrOPh}-d_6$ . While  $m/z$  95 ( $\text{C}_6\text{H}_5\text{OD}^{+\bullet}$ ) is the only ion seen in metastable ion decompositions of  $i\text{PrOPh}^{+\bullet}-d_6$ , a slight but detectable level of a lighter ion ( $m/z$  94: $m/z$  95 = 0.03) has been reported<sup>8</sup> in the ion source (where decompositions faster than  $10^6 \text{ s}^{-1}$  are sampled). Therefore, one of our objectives has been to measure the extent of this reaction under conditions where the energy content of the decomposing ions can be better assessed. The result is that isotopic scrambling cannot be detected under the experimental conditions described here. We shall argue that different mechanisms operate for primary vs secondary acyclic alkyl groups.

## Experimental Section

The TRPD experiment as applied to these ions has been outlined in a series of publications.<sup>12</sup> Briefly, the parent ion of interest is generated by electron impact ionization, trapped in an ion cyclotron resonance (ICR) cell, thermalized by collisional and radiative cooling, and photodissociated by a short (10 ns) light pulse from a laser. The appearance of photodissociation daughter ions is measured as a function of time after the laser pulse by the ion detection capabilities of the ICR spectrometer.

The ICR spectrometer and TRPD setup used in these experiments have been described.<sup>12,13</sup> Ions were produced by nominal 14 eV electrons at an ionization gauge pressure of  $3 \times 10^{-7}$  Torr of neutral compound, which corresponds to an actual pressure of about  $8 \times 10^{-8}$  Torr. They were thermalized for 3 s prior to the laser pulse, which was considered ample for collisions and radiative cooling to relax any excess internal energy and give a parent ion population thermalized at 375 K. The 6 ns laser pulse was provided by a Lumonics dye laser pumped by a HY1200 Lumonics Nd:YAG laser. Laser dyes used were LDS 698 and LD 700 dyes from Exciton Corp. Following the laser pulse the variable delay ranged over values from 2.5  $\mu\text{s}$  to 30 ms, following which the ions were excited by an ICR rf excite pulse of 20–25  $\mu\text{s}$  duration at the daughter ion frequency ( $m/z$  94, 225 kHz). Alternate light-on and light-off cycles were used and subtracted to give the light-induced daughter-ion signal. At each value of delay time, the number of cycles averaged was on the order of 100. Representative TRPD plots are shown in Figure 1.

REMPI excitation TOF mass spectra of sample in a supersonic free jet expansion were recorded in the laboratory of Professor Bryan E. Kohler at UCR using apparatus described elsewhere.<sup>7</sup> The Spectra Physics Nd:YAG-pumped dye laser was operated in "doughnut mode". The dye used in this study was Fluorescein 548 (Exciton), pumped by the second harmonic of the Nd:YAG (532 nm). Frequency doubling of the dye fundamental was performed using a Spectra Physics Model WEX-1 wavelength extender. Laser powers up to 400  $\mu\text{J}$  per pulse were examined.

$n$ -Propyl phenyl ether was prepared from 1-iodopropane and phenol as previously described.<sup>7</sup> 1,1,1,3,3,3-Hexadeuterio-2-propanol (>99.5 atom % D) was prepared by reduction of acetone- $d_6$  with  $\text{LiAlH}_4$ . Isopropyl phenyl ethers,  $i\text{PrOPh}-d_0$  and  $i\text{PrOPh}-d_6$ , were prepared from the corresponding alcohols by conversion to the corresponding tosylates and nucleophilic displacement by sodium phenoxide.  $(\text{CH}_3)_2\text{CHOC}_6\text{H}_5$ : bp 173–175  $^\circ\text{C}$ ;  $n_D^{25} = 1.4955$ . Raman spectrum (neat, 514.5 nm exciting line): 3070, 2991, 2940, 2922, 2875, 1602, 1589, 1455, 1386 (w), 1356, 1338, 1291, 1243, 1168, 1154, 1140, 1117, 1077

(12) (a) Faulk, J. D.; Dunbar, R. C. *J. Am. Chem. Soc.* **1992**, *114*, 8596–8600. (b) Dunbar, R. C. *J. Phys. Chem.* **1990**, *94*, 3283–3286. (c) Dunbar, R. C. *J. Chem. Phys.* **1989**, *91*, 6080–6085. (d) Dunbar, R. C. *J. Am. Chem. Soc.* **1989**, *111*, 5572–5576. (e) So, H.-Y.; Dunbar, R. C. *J. Am. Chem. Soc.* **1988**, *110*, 3080–3083. (f) Dunbar, R. C. *J. Phys. Chem.* **1987**, *91*, 2804–2807. (g) Chen, J. H.; Hays, J. D.; Dunbar, R. C. *J. Phys. Chem.* **1984**, *88*, 4759–4764. (h) Dunbar, R. C. *J. Phys. Chem.* **1979**, *83*, 2376–2378.

(13) Hays, J. D.; Dunbar, R. C. *Rev. Sci. Instrum.* **1984**, *55*, 1116–1119.

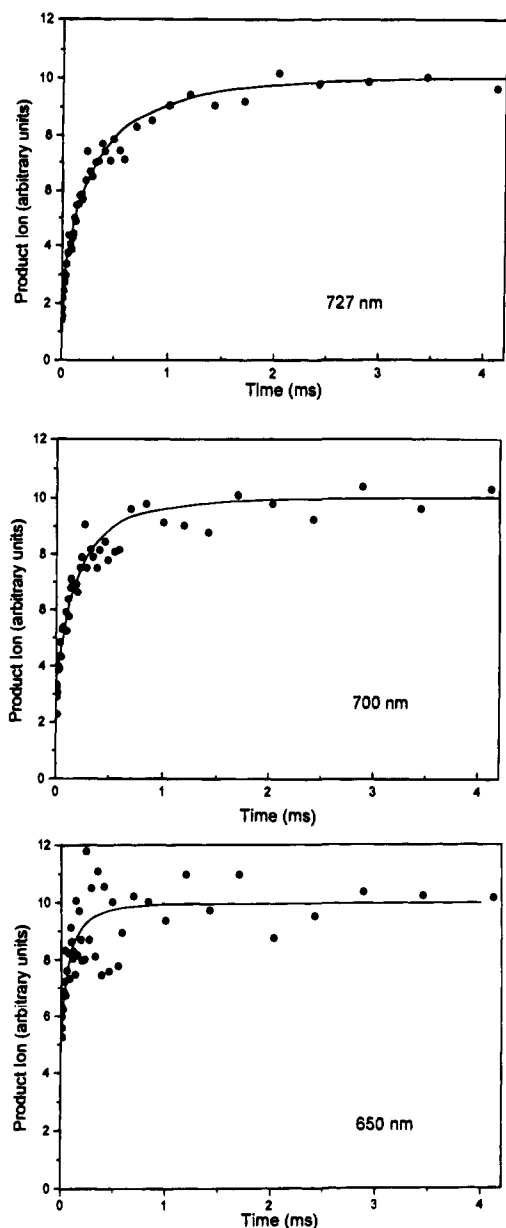


**Figure 1.** Decomposition of  $n\text{PrOPh}^+$  as a function of time following a 10 ns laser pulse at time = 0 for three different wavelengths. Solid curves represent best fit simulations.

(w), 1028, 999, 956, 861, 784, 754, 615, 598, 515, 439, 312, 236  $\text{cm}^{-1}$ .  $(\text{CD}_3)_2\text{CHOPh-}d_6$  Raman spectrum (neat, 514.5 nm exciting line): 3069, 2233, 2149, 2117, 2078, 1601, 1586, 1355, 1330, 1290, 1243, 1176, 1154, 1135, 1070, 1028, 998, 990 (sh), 878, 821, 772, 749, 718, 613, 584, 510, 429, 392, 350, 276, 234  $\text{cm}^{-1}$ . CAD mass spectra were recorded on a VG ZAB-2F double-focusing mass spectrometer using 8 kV accelerating voltage and helium collision gas.

SCF calculations were performed by means of the SPARTAN software (Version 3.0) on a Silicon Graphics 4D/35 Personal Iris computer<sup>14</sup> or GAUSSIAN (using Berny optimization)<sup>15</sup> at the San Diego Supercomputing Center. Basis set superposition error (BSSE) was assessed using counterpoise<sup>16</sup> and is taken into account in all reported values for dissociation energies  $D_e$ . Calculated SCF vibrational

frequencies were computed numerically using central differences<sup>14</sup> and are reported without use of any correction factor. For the  $C_1$  conformation of neutral  $i\text{PrOPh}$  the Hessian matrix was also calculated analytically using GAUSSIAN 92 to make sure that the normal modes do not depend on the computational method. Effects of isotopic substitution were calculated as previously described.<sup>17</sup> Large amplitude vibrations for low frequency bending modes were treated by considering them as hindered internal rotations,<sup>18</sup> and their contributions to state densities were determined by direct count.<sup>19</sup>

## Results

Propene loss represents >50% of the total ionization in 70 eV electron impact mass spectra of propyl phenyl ethers. Collisionally activated decomposition (CAD) of the  $\text{M}-\text{C}_3\text{H}_6$  ion ( $m/z$  94) from  $i\text{PrOPh}$  gives a pattern superimposable on the CAD of  $m/z$  94 from phenetole, just as has been reported for  $m/z$  94 from  $n\text{PrOPh}$ .<sup>10</sup> Since  $m/z$  94 from phenetole has the structure  $\text{PhOH}^+$  (1), we conclude that  $i\text{PrOPh}$ , like  $n\text{PrOPh}$ , does not produce 2 in appreciable amounts. Consistent with this assignment, CAD on  $m/z$  95 from  $i\text{PrOPh-}d_6$  yields, in the region of hydroxyl/water loss, only  $m/z$  77 and  $m/z$  78 fragments in a 9:1 ratio.

**Time-Resolved Photodissociation (TRPD).** The dissociation corresponding to eq 2 was readily observed for all the ions under photolytic conditions. No production of propyl ions (eq 3) or other fragments was detectable at the internal energies studied. However, the detection limit for minor photoproducts with  $m/z$  values much below that of the major decomposition peak was only about 5%. In the photodissociation of  $i\text{PrOPh}^+-d_6$  at 750 nm, the exclusive isotopic product was  $\text{C}_6\text{H}_5\text{DO}^+$  ( $m/z$  95), with <2% of  $\text{C}_6\text{H}_6\text{O}^+$ .

Three wavelengths were used for the  $n\text{PrOPh}$  experiments, giving the time-resolved data sets shown in Figure 1. In order to extract the ion dissociation rates from these plots, it is necessary to take into account the thermal distribution of parent ion internal energies and to correct for the distorting effects of the ICR detection process for fast dissociations. The procedure which we use to deconvolve the thermal distribution and the ICR detection effects has been described in considerable detail.<sup>12</sup> The results of this procedure are the dissociation rates for ions at the three photon energies (corrected by the average thermal energy content of the ions at the cell temperature of 375 K) plotted in Figure 2.

To indicate the quality of the data analysis, the simulated TRPD curves are drawn with the data in Figure 1. It is clear that the 727 and 700 nm experiments yielded excellent data and good fits to the expected curves, giving high confidence in the rates measured at these wavelengths. By comparison the 650 nm data were badly scattered and difficult to fit. In addition, there appeared to be some two-photon dissociation at this wavelength, and it was necessary to assume a nonzero contribution of daughter ions at zero time in order to obtain even a reasonable fit. These problems are reflected in a large uncertainty assigned to this rate.

The TRPD results were dramatically different for  $i\text{PrOPh}$  ions. Ample photodissociation was observed at wavelengths of 727 and 750 nm (internal energies of 2.00 and 1.95 eV, respectively), but no time dependence of the daughter ion signal was observed

(14) SPARTAN; Wavefunction Inc.: Irvine, CA. This program optimizes geometries by EF minimization, described in Baker, J.; Hehre, W. J. *J. Comput. Chem.* **1991**, *12*, 606–610.

(15) Frisch, M. J.; Trucks, G. W.; Head-Gordon, M.; Gill, P. M. W.; Wong, M. W.; Foresman, J. B.; Johnson, B. G.; Schlegel, H. B.; Robb, M. A.; Replogle, E. S.; Gomperts, R.; Andres, J. L.; Raghavachari, K.; Binkley, J. S.; Stewart, J. J. P.; Pople, J. A. *GAUSSIAN 92*, Revision B; Gaussian, Inc.: Pittsburgh, PA.

(16) Novoa, J. J.; Planas, M.; Whangbo, M. H. *Chem. Phys. Lett.* **1994**, *225*, 240–246.

(17) (a) Saunders, M.; Laidig, K.; Wolfsberg, M. *J. Am. Chem. Soc.* **1989**, *111*, 8989–8994. (b) Saunders, M.; Cline, G. W. *J. Am. Chem. Soc.* **1990**, *111*, 3955–3963.

(18) (a) Stams, D. A.; Johri, K. K.; Morton, T. H. *J. Am. Chem. Soc.* **1988**, *110*, 699–706. (b) Pacey, P. D. *J. Chem. Phys.* **1982**, *77*, 3540–3550. (c) Lewis, J. D.; Malloy, T. B.; Chao, T. H.; Laane, J. *J. Mol. Struct.* **1972**, *12*, 427–449. We are grateful to Prof. D. F. Bocian for providing us his computer code for performing these calculations.

(19) Midland, M. M.; Morton, T. H. *J. Am. Chem. Soc.* **1993**, *115*, 9596–9601.

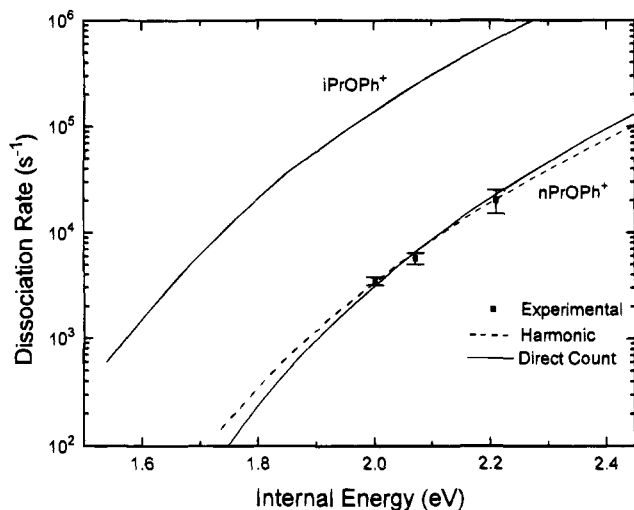


**Figure 2.** Best fit rate–energy curves for  $\text{PrOPh}^{++}$  photodecomposition (the dashed curve uses  $3N-7$  harmonic frequencies for the  $n\text{PrOPh}^{++}$  hydride shift transition state; the solid curves make use of three directly counted anharmonic vibrational modes). The  $i\text{PrOPh}^{++}$  curve is an illustrative calculation using an assumed  $E_0 = 1.33$  eV and a proton-transfer transition state.

at even the shortest delay times ( $2.5 \mu\text{s}$ ). This indicates that the  $i\text{PrOPh}$  dissociation rates at these energies are faster than  $10^5 \text{ s}^{-1}$ , taking into account the intrinsic time-resolution limitation of the TRPD experiment (primarily due, in this case, to the finite duration of the excite pulse). A similar lack of any time dependence was found for  $m/z$  95 production from  $i\text{PrOPh}-d_6$  at wavelengths of 670–750 nm. We have considered the possibility that the fast  $i\text{PrOPh}$  ion dissociation might actually be arising from two-photon dissociation. The two-photon energy of about 4 eV would undoubtedly be sufficient to give a dissociation rate greater than  $10^5 \text{ s}^{-1}$ . The characteristic signature of a two-photon dissociation is quadratic dependence of the product–ion intensity as a function of light intensity (in the limit of low extent of dissociation). An intensity dependence study at 727 nm was carried out on  $i\text{PrOPh}-d_6$  in order to test this possibility. The intensity dependence is linear, giving assurance that the observed photodissociation is a one-photon process and that  $i\text{PrOPh}$  ion dissociation is indeed faster than  $10^5 \text{ s}^{-1}$  at internal energies of as little as 1.95 eV. Two approaches have been put forth to extract activation parameters from rate–energy curves. One method assesses microscopic rate constants by means of RRKM theory by assigning vibrational frequencies to reactant and transition states.<sup>12,20</sup> In general the manner in which harmonic frequencies are varied (e.g., multiplying all frequencies by a common factor or varying a subclass of frequencies) is not important. The only important parameter appears to be the entropy of activation,  $\Delta S^\ddagger$ , which can be calculated from the assumed set of frequencies. An alternative is to assign an effective vibrational temperature for the ion and for the transition state and then to extract the activation parameters by means of a generalized Arrhenius plot.<sup>21</sup> We have chosen to make use of the RRKM approach.

The three measured rate–energy points for  $n\text{PrOPh}$  can be fitted with confidence. A straightforward RRKM calculation gives the curves drawn in Figure 2, for which the activation energy depends on whether harmonic frequencies are used (dashed line) or low frequency vibrations are treated as hindered internal rotors (solid line). Both of these approaches involve

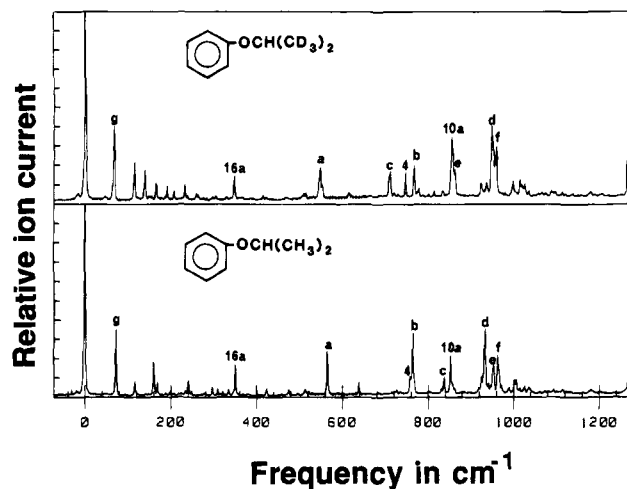


**Figure 3.** Laser/supersonic jet REMPI/TOF mass spectrometric excitation spectra of  $i\text{PrOPh}-d_6$  (top) and  $i\text{PrOPh}$  (bottom), with assignments of major peaks between 350 and 1000  $\text{cm}^{-1}$ . Modes are labeled using the numbering system of benzene<sup>25</sup>; a–f correspond to vibrations in which modes 6a, 1, and 12 are coupled to vibrations of the isopropoxy side chain.

the concurrent variation of  $E_0$  and the vibrational frequencies to find the curve most closely matching the slope and absolute values of the experimental data set. In the harmonic calculation (dashed line)  $3N-7$  harmonic frequencies were estimated for the transition state, with small variations then giving the desired fit. In the direct-count calculation (solid line) the levels of the loosest vibrational modes were generated from ab initio potentials.<sup>18,19</sup> The estimated frequencies for the harmonic, higher energy modes were grouped, varied to achieve the best fit, and combined with the fixed levels for the low-energy modes in a direct state count. The two approaches gave the same level of agreement with the experimental points, although the direct-count procedure appears to be fundamentally more satisfactory. The best fit value for the activation energy for  $n\text{PrOPh}^{++}$ ,  $E_0 = 1.47 \pm 0.02$  eV, does not show significant dependence on whether one assumes a single rate-limiting step or uses a steady-state analysis of decomposition via a transient intermediate.

**Resonance-Enhanced Multiphoton Ionization (REMPI).** Supersonic jet/REMPI experiments were performed on isopropyl phenyl ethers for two purposes. One was to test whether absorption of two photons by the lowest vibrational level of  $S_1$  gives the same mass spectrum as observed by TRPD. The other was to assess whether the two methyl groups are equivalent in the favored conformation. Figure 3 reproduces the REMPI excitation spectra. The appearance of these two spectra is similar, and most of the bands in the low energy region ( $<350 \text{ cm}^{-1}$  from the origin band, e.g., band g) can be assigned as normal modes that involve the isopropoxy group. The prominent bands between 500 and 1000  $\text{cm}^{-1}$  can be assigned to vibrational modes that involve the benzene ring, based on the Raman spectra of  $i\text{PrOPh}$  and  $i\text{PrOPh}-d_6$ , on SCF calculations, and by analogy to assignments for  $n$ -propyl phenyl ether<sup>7</sup> as well as for anisole, phenol, and alkyl-substituted benzenes.<sup>22,23</sup>

(22) (a) Balfour, W. J. *J. Mol. Spectrosc.* **1985**, *109*, 60–72. (b) Owen, N. L.; Hester, R. E. *Spectrochim. Acta* **1969**, *25A*, 343–354. (c) Murray, M. J.; Cleveland, F. F. *J. Chem. Phys.* **1941**, *9*, 129–132. (d) Bist, H. D.; Brand, J. C. D.; Williams, D. R. *J. Mol. Spectrosc.* **1969**, *24*, 402–12, 413–467.

(23) (a) Hopkins, J. B.; Powers, D. E.; Smalley, R. E. *J. Chem. Phys.* **1980**, *72*, 5039–5048. (b) Hopkins, J. B.; Powers, D. E.; Mukamel, S.; Smalley, R. E. *J. Chem. Phys.* **1980**, *72*, 5049–5061. (c) Gruner, D.; Brumer, P. *J. Chem. Phys.* **1991**, *94*, 2848–2861. (d) Takahashi, M.; Kimura, K. *J. Chem. Phys.* **1992**, *97*, 2920–2927.

(20) Riley, J.; Baer, T. *J. Am. Soc. Mass Spectrom.* **1991**, *2*, 464–469.

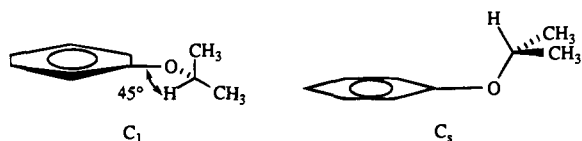
(21) (a) Klots, C. E.; *J. Chem. Phys.* **1980**, *90*, 4470–4473. (b) Klots, C. E. *J. Chem. Phys.* **1990**, *93*, 2513–2520. (c) Klots, C. E.; *J. Phys. Chem.* **1992**, *96*, 1733–1736.

The origin band of the  $S_0 \rightarrow S_1$  transition is observed at  $36\,110\text{ cm}^{-1}$  in both  $-d_0$  and  $-d_6$ . This is the most intense band, which suggests that there is not a large difference in equilibrium geometry between the  $S_1$  state and the ground state. Another, much weaker peak at  $36\,225\text{ cm}^{-1}$ , shows a smaller isotopic frequency shift than the other peaks  $<350\text{ cm}^{-1}$  from the origin and might conceivably be the origin of a second conformer. These are to be compared with the three intense origin bands reported for  $n\text{PrOPh}$  at  $36\,345$ ,  $336\,362$ , and  $36\,471\text{ cm}^{-1}$ .<sup>7</sup> Since the intensity of the putative second origin of  $i\text{PrOPh}$  is low, vibrational modes built on it cannot be easily detected. SCF calculations argue against the presence of a detectable second conformer in a supersonic free jet expansion.

In the mass spectrum the amount of isotopic label in the phenol<sup>+</sup> fragments from REMPI on  $i\text{PrOPh}-d_6$  was the same as in the TRPD experiment. At  $276.94\text{ nm}$  (the origin band) only  $\text{C}_6\text{H}_5\text{DO}^+$  ( $m/z\ 95$ ) was detected;  $\text{C}_6\text{H}_6\text{O}^+$  ( $m/z\ 94$ ) represents  $<0.015$  the intensity of  $\text{C}_6\text{H}_5\text{DO}^+$ . At higher laser powers other fragment ions are observed, but  $\text{C}_6\text{H}_6\text{O}^+$  was not observed at any laser power. Thus, we conclude that the extent of hydrogen transfer from the alkyl methine carbon under TRPD or REMPI conditions is less than half of the upper bound reported for an electron-impact ion source.

Supersonic jet spectroscopy has been widely used for conformational analysis of flexible molecules. One approach has been used to scrutinize observed vibrational progressions in detail. An alternative<sup>24</sup> has been to examine vibrational frequency shifts that accompany isotopic substitution. If the object is to distinguish two conformers, only one of which has a plane of symmetry (which is not perturbed by the isotopic substitution), then qualitative differences can be discerned in the shifts predicted *ab initio*. We surmise that shifts predicted for a ground electronic state should also pertain to an electronically excited state, provided the geometries of the two states do not differ too greatly from one another.

The conformations of  $i\text{PrOPh}$  have been explored by Hartree-Fock based SCF calculations. At 3-21G//3-21G, we find only two stable structures for the neutral molecule. The favored conformer is calculated to lie  $0.09\text{ eV}$  below the lowest conformer of  $n\text{PrOPh}$  (with zero-point energies taken into consideration). The conformer with lower electronic energy has no molecular symmetry ( $C_1$ ), with the methine carbon in the same plane as the phenoxy group, as drawn below. The other



conformer has an electronic energy  $0.1\text{ eV}$  higher and possesses a plane of symmetry ( $C_s$ ) with the methine-oxygen bond in a plane perpendicular to the benzene ring and both methyl groups equivalent. If one transposes a methyl and the methine hydrogen within the  $C_1$  conformation, optimization leads either to the  $C_s$  or returns to the stable  $C_1$  geometry. If one transposes a methyl and a hydrogen in the  $C_s$  structure, optimization leads to the  $C_1$ . UHF geometry optimizations (6-31G\*\*//6-31G\*\*) on the radical ions show that, when ionized, the  $C_s$  conformer does not retain its plane of symmetry but undergoes barrier-free internal rotation to  $C_1$ .

(24) For recent examples, see (a) Hollas, J. M. *Chem. Soc. Rev.* **1993**, 22, 371–382. (b) Song, X.; Davidson, E. R.; Gwaltney, S. R.; Reilly, I. P. *J. Chem. Phys.* **1994**, 100, 5411–5421.

(25) Varsanyi, G. *Vibrational Spectra of Benzene Derivatives*; Academic: New York and London, 1969; pp 68–78.

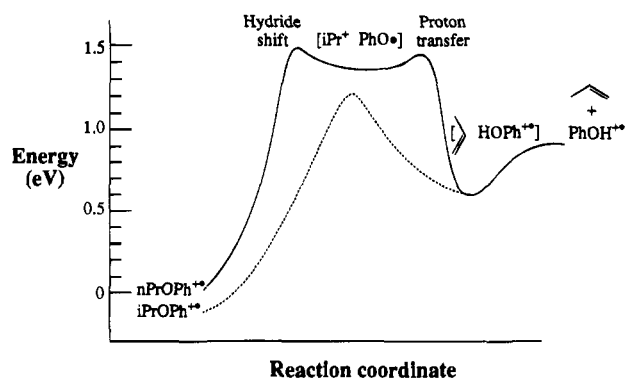


**Figure 4.** Schematic representation of the reaction coordinate for decomposition of isomeric propyl phenyl ether molecular ions with the dashed curve representing an upper bound for the  $i\text{PrOPh}^+$  dissociation barrier.

Vibrational analysis leads to the conclusion that in the gas phase the  $C_1$  conformer does indeed lie lower than the  $C_s$  (which calibrates the accuracy of the *ab initio* calculations). In our published REMPI study of  $n\text{PrOPh}$ , isotopic shifts calculated for electronic ground states were used to assign conformations, based on the vibrations observed for  $S_1$ . This was justified, in part by the fact that, of the two lower conformers, one has a planar skeleton and the other does not. The sign of the isotopically induced shift resulting from deuteration of  $\text{sp}^3$ -carbons is sensitive to the degree of planarity. We assumed this to be true of the first excited state just as it is of the ground state. In the case of isopropyl phenyl ether we focus on the band labeled **d** in Figure 3, which shifts to a higher frequency upon deuteration. This is as anticipated for the  $C_1$  conformation, while a shift to lower frequency would have been expected for the  $C_s$  conformation.

## Discussion

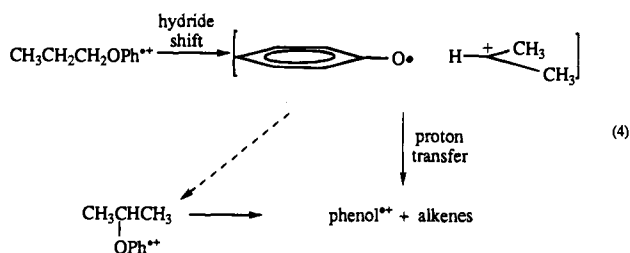
The new results presented here give insight into the mechanisms as well as the dissociation kinetics of  $\text{C}_3\text{H}_7\text{OPh}^+$ . A fairly detailed picture of  $n\text{PrOPh}^+$  dissociation will be offered, supported by computation and by the available experimental evidence. The fragmentation mechanism of  $i\text{PrOPh}^+$  is clearly different from  $n\text{PrOPh}^+$ , but we can only give a rather speculative assessment of some mechanistic possibilities.

**Dissociation Mechanism.** In addition to the thermochemical and mechanistic clues from prior work on these ions and their relatives, the present results give two types of new information about the dissociations, which must be accommodated in mechanistic proposals. The TRPD results fix the rate-energy curve for  $n\text{PrOPh}^+$  dissociation, give a fairly precise extrapolated value for the barrier  $E_0$  in the rate-determining step (whose accuracy appears to be limited only by the limitations of the RRKM model), and show that dissociation of  $i\text{PrOPh}^+$  ions with similar internal energies (around  $2\text{ eV}$ ) is much faster. The REMPI mass spectrometric results rule out transpositions of alkyl hydrogens within dissociating  $i\text{PrOPh}^+$  ions having known internal energies of around  $4.5\text{ eV}$ . This outcome is particularly interesting in contrast to the corresponding experiments in  $n\text{PrOPh}^+$ , which show randomization of the alkyl hydrogens.<sup>7</sup>

Equation 4 gives a schematic representation of the mechanistic picture that we consider to accord best with the available information. Figure 4 carries this further, proposing a quantitative reaction path for dissociation of one isomer (solid line) and an upper-bound barrier for the other (dashed line). The  $n$ -propyl isomer begins its decomposition with a hydride shift within the propyl group, more or less concurrent with breaking of the O–C bond, to give  $[i\text{Pr}^+ \text{PhO}^*]$ , an intermediate ion–neutral complex.

This intermediate transfers a proton from the isopropyl cation to the oxygen, passing through a potential well, denoted [propene  $\text{PhOH}^+$ ], *en route* to the separated products. Although the two transition states along this path both limit the net reaction rate, we conclude that the first (hydride transfer) transition state is the more severe bottleneck and can be approximately treated as the rate-determining point along the reaction coordinate.

**Thermochemical Assignments and the Potential Surfaces for Dissociation.** We start by describing the basis for assigning the energies of the various species in Figure 4. Equation 4 summarizes our understanding of the dissociation pathways for  $\text{C}_3\text{H}_7\text{OPh}^+$ . We cannot rule out collapse of the noncovalent complex [ $i\text{Pr}^+ \text{PhO}^*$ ] to the covalent structure  $i\text{PrOPh}^+$ . This is represented by the dashed arrow in eq 4, but we are at present unable to assess the extent to which the decomposition occurs *via* that route. Figure 4, which displays a potential energy curve



corresponding to eq 4, is a composite of experimental and computational results. The energies of the species along the solid curve are assigned as follows, relative to  $n\text{PrOPh}^+$  as the zero of energy.

$n\text{PrOPh}^+$  and  $i\text{PrOPh}^+$  (0 and  $-0.15$  eV). The ionization energies of the neutrals have been reported<sup>8</sup> and are no more than 0.1 eV apart. Because this difference is comparable to the experimental uncertainty, we use the same ionization energy for both isomers, 8.1 eV. The heat of formation of  $n\text{PrOPh}$  neutral has also been reported ( $-1.31$  eV),<sup>8</sup> while neutral  $i\text{PrOPh}$  is assigned as being more stable by 0.15 eV based on analogy to other ethers.<sup>26</sup>

**Hydride Shift Transition State** (1.47 eV). This transition state for  $n\text{PrOPh}^+$  is assigned a value of  $E_0 = 1.47$  eV above the  $n\text{PrOPh}^+$  ion based on the RRKM analysis of the TRPD results.

**[ $i\text{Pr}^+ \text{PhO}^*$ ] Complex** (1.35 eV). The energy of this noncovalent complex is about 0.55 eV below phenoxy radical plus isopropyl cation (whose heats of formation are reported to be 0.42<sup>27</sup> and 8.28 eV,<sup>28</sup> respectively) based on an UHF calculation using the 6-31G\*\* basis set.

**Proton Transfer Transition State for the [ $i\text{Pr}^+ \text{PhO}^*$ ] Complex** (1.43 eV). The barrier to proton transfer (0.08 eV above the ion–neutral complex) was taken to be equal to the value that we have computed at 6-31G\*\* for [ $i\text{Pr}^+ \text{NH}_3$ ]  $\rightarrow$   $\text{NH}_4^+$  and propene<sup>29</sup> (a 0.14 eV SCF electronic energy difference minus the zero-point energy correction). That calculated transition state has an SCF electronic energy 1.0 eV higher than the [propene  $\text{NH}_4^+$ ] complex at 6-31G\*\*//6-31G\*\* (a gap that is

0.05 eV greater than has been reported for a 6-31G//3-21G calculation<sup>30</sup>).

**[Propene  $\text{HOPh}^+$ ] complex** (0.7 eV). The binding energy  $D_0$  of this noncovalent complex (0.18 eV) was taken equal to the value we have calculated for the [ $\text{NH}_4^+$  propene] complex.<sup>29</sup>

**$\text{PhOH}^+ + \text{Propene}$**  (0.90 eV). The heats of formation of the dissociation products are well known, lying 0.9 eV above the  $n\text{PrOPh}^+$  reactant ion.<sup>8</sup> Thus, the thermochemical threshold for the isopropyl isomer dissociation is 1.05 eV.

**Hydrogen Randomization.** The thermodynamic threshold for producing phenol<sup>+</sup> and propene from  $i\text{PrOPh}$  at room temperature corresponds to the absorption of two 270 nm photons. Because the origin band of  $i\text{PrOPh}$  happens to occur at a longer wavelength, REMPI at 276.94 nm cannot produce  $i\text{PrOPh}^+$  with enough internal energy to fragment. Thus propene expulsion in the REMPI mass spectrum requires an additional photon. Absorption of the third photon by  $i\text{PrOPh}^+$  corresponds to an internal energy of the ion  $\geq 4.5$  eV. It is notable that this high-energy dissociation of  $i\text{PrOPh}^+ - d_6$  proceeds without detectable transposition of isotopic label. In contrast, previous REMPI results indicate randomization of all seven side chain hydrogens in high-energy dissociations of the  $n$ -propyl isomer  $n\text{PrOPh}^+$ . This is in contrast to metastable ion dissociations (2.5 eV),<sup>6</sup> where six hydrogens randomize, with only slight participation of the seventh.

Simple, irreversible traversal of the potential surface drawn in Figure 4 renders six alkyl hydrogens equivalent but not all seven. Therefore, a hydrogen transposition must become reversible in the high-energy dissociation of  $n\text{PrOPh}^+$ . If the  $n$ -propyl and isopropyl dissociations cross paths before the final minimum, it becomes complicated to rationalize why one isomer scrambles hydrogen and the other does not. If the two isomers proceed by completely different paths, then rearrangements within the ion–neutral complex can be invoked in the  $n$ -propyl case.

**Dissociation Mechanism for  $i\text{PrOPh}^+$ .** Figure 4 does not specify the nature of the transition state for propene expulsion from  $i\text{PrOPh}^+$ . The task in assigning a mechanism is to explain why the isopropyl isomer dissociates at least 30 times faster than the  $n$ -propyl isomer at internal energies around 2 eV and at the same time to explain why scrambling of all the alkyl hydrogens is observed for the  $n$ -propyl isomer, but not for the isopropyl isomer, at internal energies near 4.5 eV. In order for  $i\text{PrOPh}^+$  to decompose as fast as we observe,  $E_0$  cannot be greater than the range 1.3–1.4 eV. For example, Figure 2 depicts the rate–energy curve (dashed line) calculated for  $E_0 = 1.33$  eV, which fits the slowest rates consistent with the TRPD observation at 1.95 eV. The appearance energy comparison discussed below suggests that this value for  $E_0$  and the corresponding rate–energy curve may not be too far from correct. We conceive of two mechanistic alternatives (neither of which is positively ruled out by the experimental results), but the actual pathway will need to be clarified by additional work.

**Ion–Neutral Complex.** The  $n$ -propyl and isopropyl pathways could converge at the common structure [ $i\text{Pr}^+ \text{PhO}^*$ ], both proceeding from this point onward through the proton-transfer transition state discussed above. The different decomposition rates would then have to be ascribed to different transition states prior to this intermediate. This suggestion has the merit of giving a smooth and reasonable looking pathway. Its drawbacks are, first, that it implies an overestimate by several tenths of an electronvolt in our calculation of the energies of noncovalent

(26) Based on the assumption that the difference in  $\Delta H_s^\circ$  is the same as the  $\Delta H_s^\circ$  reported for  $n$ -propyl methyl ether vs isopropyl methyl ether (Domalski, E. S.; Hearing, E. D. *J. Phys. Chem. Ref. Data* **1993**, *22*, 805–1159).

(27) (a) Back, M. H. *J. Phys. Chem.* **1989**, *93*, 6880–6881. (b) Suryan, M. M.; Kafafi, S. A.; Stein, S. E. *J. Am. Chem. Soc.* **1989**, *111*, 1423–1429, 4594–4600 (in preference to the value for  $\Delta H_s^\circ$  (g) of  $\text{PhO}^*$  reported by Walker, J. A.; Tsang, W. *J. Phys. Chem.* **1990**, *94*, 3324–3327).

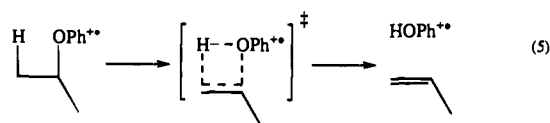
(28) Lias, S. G.; Bartmess, J. E.; Liebman, J. F.; Holmes, J. L.; Levin, R. D.; Mallard, W. G. *J. Phys. Chem. Ref. Data, Suppl.* **1988**, *17*.

(29) Audier, H. E.; Morton, T. H. *Org. Mass Spectrom.* **1993**, *28*, 1218–1224.

(30) Reiner, E. J.; Poirier, R. A.; Peterson, M. R.; Czismadia, I. G.; Harrison, A. G. *Can. J. Chem.* **1986**, *64*, 1652–1660.

complexes (otherwise the predicted rate for the isopropyl case is much too low) and, second, that it requires additional complications to the mechanistic picture in order to explain the isotope-scrambling difference between the two isomers in higher-energy fragmentations.

**Independent Pathway.** Ionized *i*PrOPh could dissociate through a transition state distinct from either of the transition states represented by the solid profile in Figure 4. This transition state cannot have an energy barrier much greater than  $E_0 = 1.35$  eV if it is to give a rate consistent with the TRPD results. This hypothesis has the drawback that no candidate transition state has yet been identified with such a low energy. Perhaps the decomposition occurs *via* "a tight four-membered ring transition state" (as suggested by Riley and Baer in their analysis of the elimination of  $C_2H_4$  from ionized phenetole<sup>20</sup>), as portrayed in eq 5. Such a suggestion invites comparison with thermal HX eliminations from neutral halopropanes ( $C_3H_7X$ ), which are the best understood examples of reactions that pass through four-member cyclic transition states.<sup>31</sup> Experimentally the activation energies for *i*PrX are about 0.2 eV lower than for the corresponding *n*PrX.<sup>31,32</sup>



**Comparison with Appearance Energy Measurements.** A quantitative test of our proposed rate-energy curves comes from electron-impact appearance energy (AE) values.<sup>8</sup> For *n*PrOPh<sup>+</sup> the rather slow rise of the rate-energy curve in Figure 2 leads to the expectation of a substantial kinetic shift; that is, the measured appearance energy should be considerably higher than the true barrier  $E_0$ . For *i*PrOPh<sup>+</sup>, the kinetic shift is less certain, because the slope of the rate-energy curve is more speculative, but it should certainly be substantial in this case as well. For both isomers the dissociation mechanisms and potential surfaces proposed here (*via* the RRKM rates derived from them) give predictions for conventionally measured fragmentation appearance energies that accord with observation.

Blanchette *et al.*<sup>8</sup> reported the appearance energy for the propene-loss channel of *n*PrOPh<sup>+</sup> to be 10.0 eV (looking at metastable ion dissociations). Using the normal criterion for the "conventional kinetic shift"<sup>33</sup> (namely the energy at which the dissociation rate exceeds  $10^3$  s<sup>-1</sup>), we can use the rate-energy curve of Figure 2 to predict a kinetic shift of 0.41 eV for this dissociation to give a value of  $E_0$  plus kinetic shift equal to 1.88 eV. From our SCF normal mode calculations we get an average thermal internal energy for  $C_3H_7O^+$  of 0.17 eV at room temperature. Taking the ionization energy of *n*PrOPh as 8.1 eV<sup>8</sup> (and assuming that the ion has the same thermal energy as its precursor neutral) we predict an appearance energy of 9.8 eV for propene expulsion. This is in agreement with the measured 10.0 eV.

Holmes *et al.* report that the AE of the same fragment from *i*PrOPh<sup>+</sup> is substantially lower than this, 9.64 eV.<sup>8</sup> The provisional rate-energy curve for this dissociation assigned in Figure 2 (which corresponds to the dashed potential energy profile in Figure 4) extrapolates to a conventional kinetic shift of 0.25 eV (*i.e.*,  $E_0$  plus kinetic shift = 1.58 eV). Using the

same ionization energy as for *n*PrOPh (and 0.17 eV of thermal energy in the ion), we predict an appearance energy for this isomer of 9.61 eV. This is in excellent agreement with the measured value.

**Other Possible Mechanisms.** Several mechanisms can be imagined that involve initial rearrangements of one or both isomers to a common intermediate structure, which then undergoes the rate-determining dissociation to  $PhOH^{++} + C_3H_6$ . One example of such a mechanism would be the reversible, rapid interconversion of the series of distonic species portrayed in eq 6, followed by slow dissociation of the distonic ions. Such a mechanism is plausible *a priori*, since the heat of formation of *i*PrOPh is approximately 0.15 eV lower than that of *n*PrOPh,<sup>26</sup> and the less stable molecular ion might rearrange to the more stable one. However the TRPD data rule out all mechanisms of this type, for such a mechanism demands that both isomers have the same rate-limiting step (propene elimination *via* a common distonic ion structure in the particular example of eq 6). Were this the case, then photolysis of the more stable (isopropyl) radical cation would produce a distonic intermediate with less internal energy. Therefore, if distonic ions did intervene, the isopropyl-containing precursor ion should have decomposed more slowly. Since it is the *n*-propyl-containing ions that decompose more slowly at 727 nm, no mechanism can be operating which invokes as its rate-limiting step the decomposition of a common intermediate.



## Conclusion

Information available regarding propene expulsion from gaseous  $C_3H_7O^+$  includes the following results from this and previous work:

(i) The barrier for *n*PrOPh<sup>+</sup> is 0.6 eV above the thermochemical threshold. The barrier for *i*PrOPh<sup>+</sup> is  $\leq 0.3$  eV above the thermochemical threshold.

(ii) Under conditions where decomposition is faster than  $10^8$  s (*e.g.*, ions from jet/REMPI), *n*PrOPh<sup>+</sup> randomizes all of the side chain hydrogens in the course of propene expulsion. Under very similar conditions *i*PrOPh<sup>+</sup> manifests no hydrogen exchange. Under conditions of slow fragmentation with rate  $< 10^5$  s<sup>-1</sup> (metastable ion fragmentation) there is little or no scrambling of sidechain hydrogens in *n*PrOPh<sup>+</sup> beyond what would be expected for isomerization of the *n*-propyl to an isopropyl.

(iii) CAD on the propene expulsion fragment ions from isomeric  $C_3H_7O^+$  ions all give the same pattern, which implies that they all have the structure  $PhOH^{++}$ .

(iv) If Hartree-Fock-based calculations are to be believed (both those presented here and elsewhere),<sup>34</sup> none of the stable aggregates of isopropyl cation with phenoxy radical is to be placed less than 1.5 eV above *i*PrOPh<sup>+</sup>. Such a high barrier to dissociation is hard to reconcile with the observed TRPD dissociation rate and with the observed appearance energy for the fragmentation, indicating the likelihood of a fundamentally different dissociation pathway for this isomer.

We have not been able to find a plausible intermediate on the pathway for *i*PrOPh<sup>+</sup> dissociation for which RRKM theory predicts a rate anywhere near as large as  $10^5$  s<sup>-1</sup>. We are left with the supposition that proton transfer might occur concomitantly with bond cleavage in *i*PrOPh<sup>+</sup>. Such a mechanism would have to be qualitatively different from 4-center eliminations that have been reported in other ions, where the barrier

(31) (a) Benson, S. W.; Bose, A. N. *J. Chem. Phys.* **1963**, *39*, 3463-3475. (b) Tschuikow-Roux, E.; Maltman, K. R. *Int. J. Chem. Kinet.* **1975**, *7*, 363-379, and references therein.

(32) Okada, K.; Tschuikow-Roux, E.; Evans, P. J. *J. Phys. Chem.* **1980**, *84*, 467-471.

(33) Huang, F. S.; Dunbar, R. C. *J. Am. Chem. Soc.* **1990**, *112*, 8167-8169. Faulk, J. D.; Dunbar, R. C. *J. Phys. Chem.* **1991**, *95*, 6932-6936.

(34) Berthomieu, D.; Brenner, V.; Ohanessian, G.; Denhez, J. P.; Millié, P.; Audier, H. E. *J. Am. Chem. Soc.* **1993**, *115*, 2505-2507.

heights are considerably in excess of the thermodynamic threshold and large kinetic energy releases are reported.<sup>35</sup> RRKM modeling indicates a dissociation barrier for *i*PrOPh<sup>+</sup> no greater than 1.35 eV but does not give a definite value. Supposing a fairly loose (proton-transfer) transition state and  $E_0 = 1.33$  eV, we expect the *i*PrOPh<sup>+</sup> decomposition rate to move into a range measurable by TRPD ( $<10^5$  s<sup>-1</sup>) for photolysis energies just below the longest wavelength used in the present study (750 nm).

Despite nearly 3 decades of intense scrutiny alkene expulsions from molecular ions of simple alkyl phenyl ethers continue to pose a number of yet unanswered questions. We surmise that it might be possible to discern these various stages of rearrangement and hydrogen transposition by means of wavelength dependence of isotopic scrambling in future TRPD studies. We foresee that a combination of neutral product studies and TRPD experiments will enlarge our understanding and provide a paradigm for unimolecular ion decompositions.

**Acknowledgment.** We are grateful to Professor B. E. Kohler for the use of his jet-REMPI apparatus and to Dr. Viet Nguyen

for performing CAD studies. This work was supported by grants from the NSF (CHE 91-16155 and CHE 92-03066) and the NIH (EY 06466). R.C.D. acknowledges with gratitude the support of the National Science Foundation (CHE 91-22333) and of the donors of the Petroleum Research Fund, administered by the American Chemical Society.

**Supplementary Material Available:** Assignment of peaks in the REMPI spectra, details of RRKM calculations, and details of ab initio estimates (9 pages). This material is contained in many libraries on microfiche, immediately follows this article in the microfilm version of the journal, and can be ordered from the ACS; and can be downloaded from the Internet; see any current masthead page for ordering information and Internet access instructions.

JA9419019

---

(35) Cacace, F.; Grandinetti, F.; Pepi, F. *Angew. Chem. Int. Ed. Engl.* **1994**, *33*, 123–125.